Library Progress International
Vol.44 No.3, Jul-Dec 2024: P. 26397-26416

Print version ISSN 0970 1052
Online version ISSN 2320 317X

Original Article

Available online at www.bpasjournals.com

OPTIMIZATION OF HPDC PARAMETERS FOR AlSi9Cu3 ALLOYS THROUGH THE UTILIZATION OF DESIGN OF EXPERIMENTS (DOE) FOR POROSITY AND STRENGTH ENHANCEMENT

[1]Vinod Kumar Verma, [2]*Sanjeev Sharma, [3]Sandeep Phogat, [4]Ajay Kumar Mishra, [5]PB Sharma

[1]Research Scholar, Department of Mechanical Engineering, Amity University Gurugram Haryana 122412, India. Email id: vinod2005verma@gmail.com
[2]Professor, Department of Mechanical Engineering, Amity University Gurugram Haryana 122412, India. Email id: ssharma26@ggn.amity.edu
[3]Assistant Professor, Department of Mechanical Engineering, Amity University Gurugram Haryana 122412, India. Email id: sandeepphogat1@gmail.com
[4]Professor Director Academy of Nanotechnology, University of South Africa, Florida Science Campus Johannesburg, South Africa. Email id: ajaykmishra1@gmail.com
[5]Professor Vice Chancellor, Amity University Gurugram Haryana 122412, India. Email id: pbsharma@ggn.amity.edu

How to cite this article: Vinod Kumar Verma, Sanjeev Sharma, Sandeep Phogat, Ajay Kumar Mishra, PB Sharma (2024) OPTIMIZATION OF HPDC PARAMETERS FOR AlSi9Cu3 ALLOYS THROUGH THE UTILIZATION OF DESIGN OF EXPERIMENTS (DOE) FOR POROSITY AND STRENGTH ENHANCEMENT. Library Progress International, 44(3), 26397-26416

ABSTRACT

Purpose: Through the optimization of High Pressure Die Casting (HPDC) parameters, the quality and effectiveness of AlSi9Cu3 castings are to be enhanced in this study.

Method: Using Design of Experiments (DOE), the effects of important HPDC parameters, including injection speed, mold temperature, and pressure, were investigated. To determine the ideal parameters, the study utilized multivariable linear regression (MVLR) and genetic algorithm (GA) approaches. The L27 orthogonal array from the Taguchi method was utilized in the experiments, along with MVLR modeling to identify process correlations and GA for optimization. Key parameters were also changed.

Result: The process successfully determined the ideal HPDC settings, resulting in the lowest porosity in the castings of AlSi9Cu3. The validity of the approach was proved by comparing the projected and real data.

Conclusion: The HPDC process quality was greatly enhanced by the combined application of DOE, GA, and MVLR approaches, providing a workable way to raise casting performance and efficiency.

Keywords: Aluminium die casting, Porosity, High Pressure Die Casting, $AlSi_9Cu_3$ alloys

INTRODUCTION

High-pressure die casting technology is in widespread use in the industry because of its high productivity and the minimal requirement for post-machining. The lightweight and exceptional forming properties of aluminum die casting make it a popular choice to produce automotive and transportation components [1]. In addition to being a more economical and effective way to produce components with minimal surface roughness and high dimensional precision, it offers a considerably higher production rate than alternative technologies [2]. Aluminum can be employed in this manner to fabricate all essential auto components. The industrial sector has become reliant on computer-aided simulation because of the widespread use of industrial die-casting and the increasing demand for

products with more complex geometry, faster development periods, and superior quality.

The cold chamber dies casting process's productivity and quality will be enhanced by the development of the Taguchi method control in conjunction with experiment design [3]. To determine the ideal parameters for improving the efficiency and quality of aluminum die casting, important factors are chosen for the process after a series of preliminary experiments are carried out in a controlled setting [4].

The failure of high-pressure die casting of ADC12 aluminum alloys is frequently caused by porosity, which is a consequence of rough metal flow during the cavity filling process, which captures air, gas, and oxides [5].They categorize the flaws into three categories: shrinkage porosity, which occurs when the metal hardens in the gate before solidifying in other areas of the casting; flow porosity, which occurs when the cavity filling is insufficiently pressured; and gas porosity, which occurs when air is trapped in the sleeve. Porosity in castings has an impact on their mechanical properties and pressure. The part geometry and casting parameters used during the process influence the porosity of high-pressure die casting [6]. Several distinct processes and factors influence the development of porosity. This study looks at how different process variables affect the amount of porosity in die castings of the aluminum alloy ADC12 and how to stop porosity from growing. They planned the experiments using the Taguchi parameter design approach [7–13]. The HPDC process's ideal parameter set is chosen to reduce the formation of porosity [14–16].

Figure 1 is most likely a shoulder harness restraint rather than a child mounting figure. It is a safety device used in car seats and airplane seats to restrain a child. It typically consists of two shoulder straps that connect to a buckle in the front. These holes would be used to thread the shoulder straps through.
Here are some of the safety features of shoulder harness restraints:

- They help to distribute crash forces evenly across the child's body.
- They help to prevent the child from being ejected from the seat in a crash.
- They help to keep the child's head and neck from moving too far forward in a crash.

Shoulder harness restraints are an important part of child safety in cars and airplanes. They should always be used according to the manufacturer's instructions.

Figure 1: Casting Component

Figure 2 seems to show a section of porous material that has been cut, presumably metal, and is labeled as "Cut Section Porosity Level-2." A material's porosity is a measurement of the vacant spaces inside it, represented as a percentage of the material's total volume occupied by these gaps. Porosity can affect a material's other qualities

and weaken it in the context of materials engineering. Level 2 can represent a material having a moderate porosity level. Here are some of the ways that porosity can affect the properties of a material:

- Strength: Porosity can reduce the strength of a material by reducing the amount of solid material available to carry a load.
- Stiffness: Porosity can make a material less stiff, or more prone to bending or deformation under stress.
- Density: Porous materials are less dense than non-porous materials.
- Conductivity: Porosity can reduce the thermal conductivity and electrical conductivity of a material.
- Fluid flow: Porous materials can allow fluids to flow through them. The size and distribution of the pores can affect the rate of fluid flow.

Figure 2: Cut Section Porosity Level-2

Cut section porosity refers to air pockets or holes within a cast or molded object. These holes can be caused by shrinkage of the material as it cools, by trapped air or gas, or by impurities in the material. The level of porosity is typically measured on a scale, with level 1 being the least porous and level 5 being the most porous. Level 3 porosity is a moderately high level of porosity in figure 3. It may reduce the strength and durability of the object, and it may also allow fluids to leak through. If you are concerned about porosity in a cast or molded object, you should consult with a professional to determine if it is acceptable for the intended application.

Figure 3: Cut Section Porosity Level-3

Figure 4: Cut section Porosity Level-4

Porosity refers to the number of empty spaces or voids within a material. In castings, porosity is caused by air or gas bubbles that become trapped in the metal during solidification. The level of porosity is determined by the size, number, and distribution of the pores. Level 4 porosity is considered the most severe, with pores larger than 100 micrometers and a measured volume fraction of about 10% in figure 4. The mechanical qualities of the aluminum, including its tensile strength and fatigue resistance, may be considerably weakened by these big pores. There are several techniques that can be used to reduce porosity in castings, such as proper melting practices, pouring temperature control, and vacuum degassing.

2. REVIEW OF LITERATURE

[16] conducted Products produced using all production processes have certain flaws. These flaws must be minimized to provide customers with high-quality items. Reducing flaws in final items that reach customers is the driving force behind this endeavor, which will boost productivity. The goal of this project is to minimize component rejections caused by blowhole defects that occur during the High Pressure Die Casting process. The aluminum alloy rack housing is the preferred casting product for this inquiry (ADC 12). This housing is fastened to the steering column of a car. Phase-1 and phase-2 velocity, intensity pressure, intensification pressure, and limit switch position were the process parameters that were investigated. For the parameters under investigation, the response factor is the casting density. Using the Taguchi parameter design approach, the process parameters are optimized. In a series of experiments, the selected process parameters were modified using the Taguchi approach. The L25 orthogonal array serves as the studies cornerstone. There is a set quantity contributed to each process component. The optimal processing parameters were discovered to reduce the number of blowholes in the ADC 12 alloy's HPDC. To reduce casting flaws, the ideal levels of process parameters for Phase-1 and Phase-2 velocity, Limit Switch Position, and Intensification Pressure have been determined using the Taguchi technique. The levels that are equivalent are 170 mm, 1 m/s, 300 kg/cm2, and 4 m/s.

[17] analyzed that the automotive industry frequently employs the casting process as a manufacturing process. Die casting is the most frequently implemented casting method. Nevertheless, it is a fact that an increasing number of industries are experiencing waste or leftovers that result from the process. Therefore, the main goal of this study is to comprehend die-casting and the factors that influence it. $AlSi_9Cu_3$ is the raw material utilized to produce the throttle body, which is the subject of this study. This section's primary source of worry is the prevalence of flaws such poor filling, heat bubbles, and porosity. Optimizing the process is therefore essential. To carry out the optimization, design of experiments, ideation, numerical simulations, and quality tools are utilized. The simulation uses three sets of trials, while the Taguchi orthogonal array in Minitab 18 is produced using eighteen sets of experiments. One uses Minitab to determine signal-to-noise ratios. This ratio computation is based on the "smaller the better" premise, and the response variable is the rejection %. As tools for figuring out the porosity distribution, the filling time and total shrinkage were used. Following their implementation, these measures allowed the aggregate scrap percentage to drop from 14% to 9%.

[18] conducted that an investigation into the quality of high pressure die casting commodities is a challenge that both large and small manufacturers of HPDC products encounter. Optimization of the parameters of the die casting procedure has been attempted. Through an experimental investigation, the die casting process parameters for aluminum alloys ADC12 were optimized. The goal of the inquiry was to lower the porosity of the aluminum alloy components made of ADC12 to aid in the manufacturing of high-quality castings. The most prevalent defect in high pressure die castings of aluminum is porosity, which decreases productivity and increases the likelihood of rejection and refusal. The parameters of the die casting process have a direct correlation with the development of porosity. The aim of this investigation was to decrease porosity by analyzing the impact of process factors on the porosity formation in HPDC of ADC12 alloys. The Taguchi parameter design approach was employed to modify process parameters. The Taguchi technique was used to conduct experiments, which entailed changing specific process parameters at different phases. To ascertain the importance of the parameters in the development of porosity in die castings. The findings showed that a few key process parameters significantly affect how porosity forms. The best processing conditions were found for the ADC12 alloy's HPDC porosity to be as low as possible.

[19] investigated that this study offers a thorough examination of the challenges associated with the development and application of predictive models intended to lower waste related to porosity and improve the quality of aluminum die castings. Fuzzy systems improved by simulated annealing and genetic algorithms are used to assess the porosity of casting components. The complex process of high pressure die casting is influenced by a multitude of process variables, which can result in porosity and other casting defects. This investigation illustrates the porosity of the casting components in terms of counter pressure, first and second chilling periods, first phase velocity, first phase length, and second phase velocity. The die casting porosity fuzzy systems that were created using GA and SA were demonstrated to have remarkably good prediction power. The investigation's second goal was to determine which process variable combination would result in the lowest level of porosity feasible in high-pressure die casting. For this purpose, simulated annealing and a genetic algorithm were used. Castings with the lowest practical porosity % were created after the optimal parameters were validated experimentally.

[20] conducted that casting operations are dependent on a multitude of input parameters to ensure their effectiveness. To produce castings with high productivity and no defects, a meticulous assessment of the optimal configurations of process parameters is necessary. The goal of this investigation is to enhance the efficacy of the squeeze casting, continuous casting, and die casting processes by optimizing process parameters through the application of the Jaya algorithm. The modified Jaya algorithm now incorporates pseudo-oppositional learning. The Jaya and QO-Jaya algorithms are employed to identify and rectify the optimization issues associated with each of the casting processes that have been previously discussed. The GA, SA, PSO, and TLBO algorithms are then compared to these results.

[21] investigated the most widely used technique for producing aluminum castings is high pressure die casting because it offers the best possible balance between cost and characteristics for large-scale manufacturing. Approximately 70% of the components manufactured by HPDC are composed of the most frequently employed aluminum alloy, AlSi $_9Cu_3$. $AlSi_9Cu_3$ Compounds despite this, the composition of the alloy and the intrinsic porosity of HPDC castings limit the mechanical qualities that can be achieved with standard $AlSi_9Cu_3$ alloys. To enhance these elements, new alloys and technique modifications have been created recently. The silicon alloying element in $AlSi_9Cu_3$ (Fe) EN-AC 46000 can range from 8 to 11%, with the alloying elements in $AlSi_9Cu_3$ standards varying considerably. Hardness, tensile strength (T.S.) of 240 MPa, yield strength (Y.E.) of 140 MPa, and elongation (E) of less than 1% are the standard qualities for HPDC. The goal of the present endeavor is to develop novel alloys that are comparable to $AlSi_9Cu_3$ alloys but possess specific characteristics that are tailored to meet the specific requirements. Within certain composition ranges, it is possible to improve these characteristics as well as elongation, yield strength, ultimate tensile strength, and hardness. According to its cast qualities, the alloy has a Y.S. > 200 MPa, T.S. > 320 MPa, E > 1%, and Hardness > 135 HB.

[22] conducted that this study offers the results of a quantitative investigation of the gas content of a wide range of castings made using the vacuum fusion method in the high pressure die casting procedure. The air trapped

during cavity filling was found to make up most of the gas. There were other obvious causes as well, such as air trapping during ladling, quenching water, and remaining die lubrication. The gas concentration was determined to be unequally distributed through the measurement of a large casting and castings from a multi-cavity die. As per the results, the modified vacuum fusion method can be effectively employed to determine the gas content in castings, evaluate and monitor it, and investigate the impact of various process factors on the gas's evolution over time.

Table 1: Comparison of review

Study	Focus	Findings
[16]	Reducing blowhole defects in HPDC process for aluminum alloy rack housing (ADC 12).	Optimized process parameters: Limit Switch Position: 170 mm, Intensification Pressure: 300 kg/cm², Phase-1 Velocity: 1 m/s, Phase-2 Velocity: 4 m/s... Reduced casting defects through the application of the Taguchi method.
[17]	Die casting process optimization for throttle body production using $AlSi_9Cu_3$ alloy.	Overall scrap percentage was lowered from 14% to 9% with the use of quality tools, DOE, numerical simulations, and brainstorming. Porosity distribution calculated using filling time and total shrinkage.
[18]	Optimizing die casting process parameters to minimize porosity in ADC12 aluminum alloy.	Identified significant process parameters affecting porosity. Optimized parameters using Taguchi method to achieve minimal porosity in HPDC of ADC12 alloy.
[19]	Predictive models for minimizing scrap due to porosity in aluminum die castings.	Developed predictive models using fuzzy systems improved by GA and SA. Achieved excellent predictive power for porosity. Optimized process parameters using GA and SA, resulting in castings with minimal porosity.
[20]	Optimizing casting process parameters using the Jaya algorithm and its variation.	Die casting, squeeze casting, and continuous casting procedures were optimized by employing the Jaya and QO-Jaya algorithms. The GA, SA, PSO, and TLBO algorithms were employed to compare the associated results. Improved efficiency and defect reduction in casting processes.
[21]	Enhancing the mechanical properties of the $AlSi_9Cu_3$ alloy in the HPDC process.	Developed innovative alloy compositions to enhance elongation, ultimate tensile strength, yield strength, and hardness. Achieved improved cast characteristics compared to standard $AlSi_9Cu_3$ alloys.
[22]	Quantitative study of gas levels in various types of HPDC castings using a vacuum fusion method.	Identified air trapped during cavity filling as the major source of gas. Used modified vacuum fusion method to measure gas concentration and evaluate process parameters affecting gas evolution in castings.

3. RESEARCH METHODOLOGY

High-performance and high-precision apparatus were required to ensure the accurate measurement of die casting parameter values during the experimental process. Consequently, a robotic die casting cell was established, which was automated and equipped with all requisite instrumentation, data collection, and control systems. An automatic metal input system, a holding furnace, an extractor robot with four directions of motion, a 280 t locking force die casting machine, an oil unit with programming, and a data collection and monitoring system are all components of a die casting cell. Its objective is to evaluate and investigate the relationships between various die casting attributes. Composed of the aluminum alloy $AlSi_9Cu_3$, the test specimen was a rectangular plate with dimensions of 150 by 100 by 20 mm. The entry portal measured 100 mm by 2.5 mm, while the shoot sleeve had

a diameter of 50 mm. The chemical composition of the aluminum alloy as it was used in the experiment. The die was constructed and designed with the purpose of mounting sensors, such as pressure transducers, position and velocity sensors, and thermocouples. It is manufactured using a hot work instrument made of steel AISI H11. Real-time monitoring and recording of the parameters of the die casting machine were implemented. Three casts were generated for each trial scenario using randomization. The casting density was determined through the immersion technique. The castings were weighed twice: once while submerged in entirely degassed distilled water and again while in the air. Mettler balances, which possess an accuracy of 0.0001 grams, were employed to conduct each weighting. The theoretically logical casting was anxiously anticipated. At temperatures that were marginally lower than the 510 C eutectic temperatures, cylindrical samples of the aluminum alloy AlSi9Cu3 were pulverized into powder-forming dies. The average density of the compressed samples was 2.75 g/cm3. The relationship was subsequently employed to determine porosity.

$$\text{Porosity}(\%)=(1-\rho_1./\rho_0).100$$

3.1 Taguchi design

The elements that were found to be most important in the experimental design were the die, the first and second stage plunger velocities, the third stage doubled pressure, and the preservation of the furnace's temperature. Throughout the entire experiment, the other parameters remained unchanged. The holding furnace temperature range was chosen to be 655–700 C, the die temperature range to be 195–245 C, and the plunger velocity range to be 0.03–0.43 m/s for the first stage and 2.5–3.1 m/s for the second stage. Furthermore, the third stage's double pressure range of 185–285 bars was selected. Table 2 lists the chosen casting process parameters and their respective ranges.

The Taguchi technique is a highly effective method for reducing costs and time expended, as well as improving the efficiency of processes and products, and resolving issues. The Taguchi method is founded on matrix experiments. The unique orthogonal arrays of the experimental matrices allow for the efficient investigation of the multiple effects of process factors at the same time. An orthogonal experiment aims to ascertain the ideal concentration of each element and the relative importance of each factor about its main effects on the response. Taguchi suggests that the goal function in matrix experiments be the signal-to-noise ratio to use variance analysis to identify the critical process parameters and quality features. To assess how the process components' non-linearity affected the current investigation, five parameters were defined and examined at three distinct levels. For every selected parameter with a distinct number of levels (ln), an orthogonal array is first chosen to begin the Taguchi optimization procedure. Utilizing, the array's minimum trial count is determined.

$$N_{min}=(l_n-1)p_n+1$$

where the parameter count is represented by pn. Consequently, the L27 orthogonal array was selected in accordance with the Taguchi quality design approach, resulting in $N_{min} = 11$. Each set of experiments will be run three times using this strategy to get a more accurate result. The multivariable linear regression approach uses the results of the orthogonal array experiment as training data. Table 3 is a collection of porosity values for the castings made under different conditions.

3.2 Process parameters optimization using MVLR and GAs methods

Process optimization seeks to limit porosity as much as possible by identifying the best control factors for the aluminum die casting process. The MVLR model was the source of the fitness function that was implemented during the optimization procedure in this study. This process involved the application of GAs to optimize the process conditions.

3.2.1 Multivariable linear regression analysis

Process variables are anticipated and modeled in the industrial sector using the multivariable linear regression analysis model. It is occasionally combined with other methodologies, such as genetic algorithms, decision support systems, and artificial neural networks.

3.2.2 Genetic algorithms (GAs)

The natural genetic system replicates the principles of biological evolution using genetic algorithms, which are search algorithms. Generalized alternating systems, or GAs as they are occasionally referred to, are advantageous for resolving problems that involve objective functions that exhibit "bad" properties, such as being non-differentiable, discontinuous, or multi-modal. To oversee and modify a population of solutions and seek out superior ones, these algorithms implement the "survival of the fittest" principle. GAs investigates each region of the stage space and takes advantage of prospective locations to address both linear and nonlinear problems by employing mutation, crossover, and selection procedures on population members. For everyone in the population to be represented chromosomally, the GAs must be used. Gene sequences that are descended from a certain alphabet are called chromosomes. Symbols, integers, floating point numbers, binary numerals, matrices, and other data types may all be employed in an alphabet. The representation technique establishes the genetic operators to employ and the structure of the problem within the GA. Natural representations work better in this experiment and yield better outcomes. For this reason, we see a chromosome as a vector of values that are floating points that fall between the upper and lower boundaries of the variable. With every gene acting as the issue variable, the chromosomal length functions as the vector length of the solution. Making ensuring the gene values are inside the range of the variable they represent is a need for the genetic operators.

In a GA, the selection of individuals to generate subsequent generations is crucial. Selection is the process by which two people are chosen as "parents" from the entire population of people, and it is based on each person's fitness function. Multiple selection strategies exist. The roulette wheel selection was applied in this essay. This choice represents a roulette wheel where each segment's area is proportionate to its expected value. Then, using a random number and an area-based chance, the software chooses one of the pieces. It is feasible to create children in the next generation that are different from their parents but still have traits in common with them by using genetic operators. Numerous applications exist for these operators. The two operators that are used the most are mutation and crossover. The population's chromosomes are commonly shown as binary sequences. A common term for chromosomal implementation is "encoding technique."

4. RESULT AND DISCUSSION

Table 2 presents a set of process parameters for a particular manufacturing process, together with the corresponding ranges and values at three different levels. Table 2 is organized into various categories, each of which corresponds to a particular process parameter (PP), as well as the corresponding process ranges (PR), units of measurement (UOM), and values at three different levels (Level-1, Level-2, and Level-3).

- Category A focuses on the Holding Furnace Temperature, measured in degrees Celsius (°C). The process range for this parameter is between 655 and 700C°. The specific values are 655C° at Level-1, 678C° at Level-2, and 700°C at Level-3.
- Category B deals with the Die Temperature, also measured in degrees Celsius (°C). The acceptable range for this parameter is 195 to 245C°. The defined levels are 195°C for Level-1, 220°C for Level-2, and 245 C° for Level-3.
- Category C specifies the Plunger Velocity during the 1st Stage, with units in meters per second (m/s). The velocity range is from 0.03 to 0.43 m/s. The values are 0.03 m/s at Level-1, 0.23 m/s at Level-2, and 0.43 m/s at Level-3.
- Category D covers the Plunger Velocity during the 2nd Stage, also measured in meters per second (m/s). For this parameter, the process range is 2.5 - 3.1 m/s. For Level-1, 2.8, and Level-3, the comparable speeds are 2.5, 2.8, and 3.0 m/s, respectively.
- Category E pertains to the Multiplied Pressure during the 3rd Stage, measured in bars (Bar). The pressure range is 185 to 285 Bar. The specific levels are 185 Bar at Level-1, 245 Bar at Level-2, and 285 Bar at Level-3.

The table 2 presents an organized overview for the purpose of regulating and optimizing the manufacturing process. It includes the essential process parameters, their measurement units, and the required ranges and levels.

Table 2: Process parameters with their ranges and values at three levels

Category	PP	UOM	PR	Level-1	Level-2	Level-3
A	Holding furnace temperature	C˚	655-700	655	678	700
B	Die temperature	C˚	195-245	195	220	245
C	Plunger velocity 1st stage	m/s	0.03-0.43	0.03	0.23	0.43
D	Plunger velocity 2nd stage	m/s	2.5-3.1	2.5	2.8	3.0
E	Multiplied pressure 3rd stage	Bar	185-285	185	245	285

As a means of assessing a material's porosity levels in relation to ASTM E 505 criteria, table 3 displays the findings of a Taguchi orthogonal array parameter design. Trials 1 through 27 evaluate how different parameters affect porosity. The variables include the Mould Pressure (MP) in bars, the Heat Fusion Temperature (HFT) and Discharge Temperature (DT) in degrees Celsius, and the Primary Vent Speeds 1 and 2 (PVS-1) and PVS-2 in meters per second. It took eight shots for each trial. Sample porosity is stated in levels, with Level 01 being the lowest porosity and Level 04 representing the largest porosity. Trials 1 through 3, for example, with HFT of 655˚C and DT of 195˚C with different PVS-1, PVS-2, and MP values, all produced Level 02 porosity, suggesting a rather consistent result under these conditions. Interestingly, there were little differences observed when the DT was raised to 220˚C and 245˚C under comparable circumstances. In fact, some of the trials revealed Level 03 porosity. It's interesting to see that porosity levels varied considerably when HFT was raised to 678˚C. Trial 11, with HFT of 678˚C, DT of 195˚C, PVS-1 of 0.23 m/s, PVS-2 of 3 m/s, and MP of 185 Bar, produced the greatest porosity level in this investigation, Level 04, for instance. Nevertheless, lower porosity levels were seen in other trials at this HFT, such as Level 01 in trials 10, 12, and 15. This implies that although porosity may increase with a larger HFT, PVS and MP also have a major impact on the outcome. Again, there were conflicting results at the maximum HFT of 700˚C. Low porosity levels (Level 01) were seen in certain studies, whereas Level 04 was reached in others, demonstrating the intricate relationship between these factors. Trial 19 (same HFT and DT, with PVS-1 of 0.03 m/s, PVS-2 of 3 m/s, and MP of 245 Bar) produced Level 01 porosity, but trial 21 (HFT of 700˚C, DT of 195˚C, PVS-1 of 0.43 m/s, PVS-2 of 2.8 m/s, and MP of 185 Bar) produced Level 04 porosity. Overall, this study shows that the combination of HFT, DT, PVS-1, PVS-2, and MP has a significant impact on the material's porosity. Higher HFTs result in greater variability, whilst lower HFTs often provide more consistent and lower porosity levels. This suggests that careful control of these parameters is necessary to attain the appropriate porosity level.

Table 3: Porosity results of the Taguchi orthogonal array parameter design

Trial	HFT ˚C	DT ˚C	PVS-1 m/s	PVS-2 m/s	MP-3 Bar	# of shots taken	Porosity Status compared with ASTM E 505(LEVEL)
1	655	195	0.03	2.5	185	8	Level 02
2	655	195	0.23	2.8	245	8	Level 02
3	655	195	0.43	3	285	8	Level 02
4	655	220	0.03	2.8	245	8	Level 02

5	655	220	0.23	3	285	8	Level 02
6	655	220	0.43	2.5	185	8	Level 03
7	655	245	0.03	3	285	8	Level 02
8	655	245	0.23	2.5	185	8	Level 03
9	655	245	0.43	2.8	245	8	Level 02
10	678	195	0.03	2.8	285	8	Level 01
11	678	195	0.23	3	185	8	Level 04
12	678	195	0.43	2.5	245	8	Level 01
13	678	220	0.03	3	185	8	Level 02
14	648	220	0.23	2.5	245	8	Level 01
15	678	220	0.43	2.8	285	8	Level 01
16	678	245	0.03	2.5	245	8	Level 01
17	678	245	0.23	2.8	285	8	Level 01
18	678	245	0.43	3	185	8	Level 03
19	700	195	0.03	3	245	8	Level 01
20	700	195	0.23	2.5	285	8	Level 01
21	700	195	0.43	2.8	185	8	Level 04
22	700	220	0.03	2.5	285	8	Level 02
23	700	220	0.23	2.8	185	8	Level 4
24	700	220	0.43	3	245	8	Level 3
25	700	245	0.03	2.8	185	8	Level 04
26	700	245	0.23	3	245	8	Level 02
27	700	245	0.43	2.5	285	8	Level 03

Figure 5: Radiography Report (X-Ray) After optimization Porosity Level-1 as per ASTM E 505

Let's analyze the provided radiography report (X-ray) after optimization, indicating Porosity Level-1 as per ASTM E 505.The image depicts a radiographic inspection of a component that has undergone an optimization process. The inspection aims to evaluate the presence of porosity within the material. Based on the ASTM E 505 standard, the observed porosity level is classified as Level-1 in figure 5.

Porosity Level-1 Interpretation

According to ASTM E 505, Porosity Level-1 signifies a very low level of porosity. This implies that the material contains minimal detectable voids or gas pockets. Such a low porosity level is generally considered acceptable for most applications, as it has a minimal impact on the material's mechanical properties and overall integrity.
Given the classification of Porosity Level-1, no further action is typically required. The component can be considered suitable for its intended use without any concerns regarding porosity-related issues. While the observed porosity level is within acceptable limits, it is essential to consider the specific requirements of the application. In some critical cases, even minor porosity might be unacceptable. Therefore, it is crucial to consult the relevant material specifications and engineering standards to make a final determination regarding the component's

suitability.

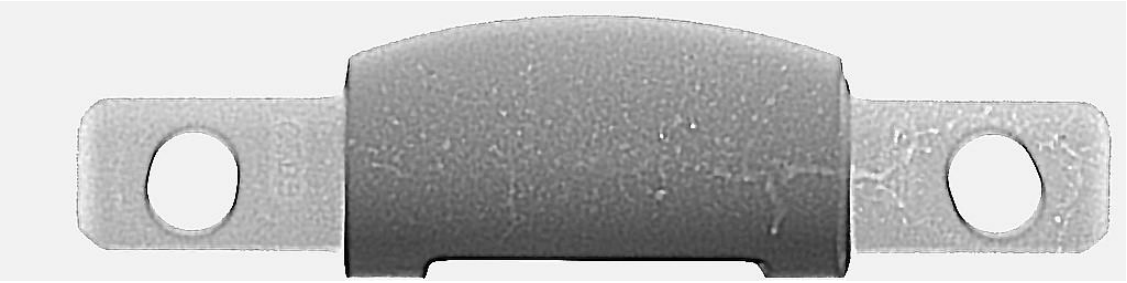

Figure 6: Radiography Report (X-Ray) Before optimization Porosity Level-3 as per ASTM E 505

The report indicates that the object was examined before an optimization process. The key finding is the presence of porosity at Level-3, as classified according to ASTM E 505 standards.

- Radiography: This non-destructive testing technique looks at a material's internal structure using X-rays. It reveals defects like voids, cracks, or inclusions that might be present within the material.
- Porosity: This refers to the presence of small holes or voids within the material. In this case, the porosity level is classified as Level-3 based on ASTM E 505 in figure 6, which suggests a moderate level of porosity.
- ASTM E 505: The American Society for Testing and Materials (ASTM) created this standard specification, which offers recommendations for assessing the porosity levels in radiographic pictures.

In summary, the radiography report indicates that the metal component in question has a moderate level of porosity (Level-3) as per ASTM E 505 standards. This information is likely crucial for assessing the component's suitability for its intended application and for implementing any necessary optimization processes.

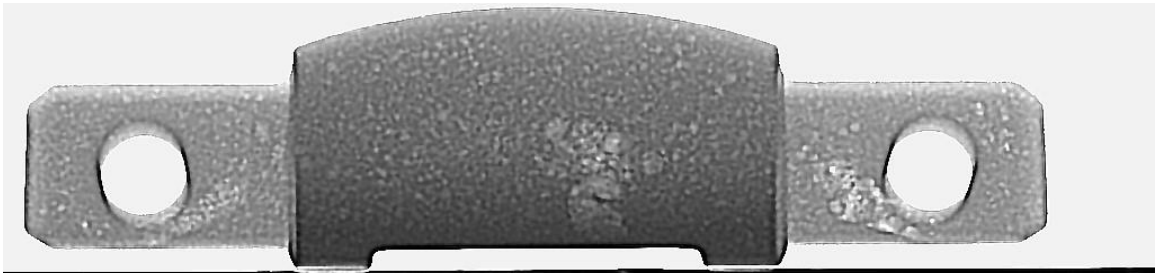

Figure 7: Radiography Report (X-Ray) Before optimization Porosity Level-4 as per ASTM E 505

Prior to optimization, present the component's radiographic report, specifically an X-ray image. The X-ray appears to have been conducted to assess the internal structure and identify any potential defects.

- Component: The central part of the image showcases the component under examination. It exhibits a metallic or dense material composition.
- Porosity: The report indicates a "Porosity Level-4" as per ASTM E 505 standard. This suggests the presence of voids or air pockets within the component's structure.
- Optimization: The mention of "Before optimization" implies that this X-ray was taken prior to any modifications or improvements made to the component.

The X-ray highlights the internal structure of the component, revealing areas of varying density. The classification of Porosity Level-4 according to ASTM E 505 in figure 7 indicates a significant level of porosity, which might be a concern depending on the component's intended application. Further analysis and potential optimization steps

would likely be undertaken to address this issue.

Data on the porosity found in a material sample prior to going through an optimization process are shown in table 4 and figure 8 and figure 9. The table lists the nine different porosities that are present in a 56 mm piece of the material. Table 4 also provides millimeter-based measures of each porosity's size. The porosities vary in size from 2.1 mm to 3.3 mm. To be more precise, the initial porosity is 2.1 mm, the second is 2.3 mm, and the third is 2.5 mm. The sizes of the fourth and fifth porosities are 2.4 mm and 2.8 mm, in that order. The sixth, seventh, and eighth porosities have respective diameters of 2.9 mm, 3.1 mm, and 3.2 mm. This sample has a maximum porosity of 3.3 mm. The purpose of this pre-optimization data is to provide a baseline against which any optimization procedures used to lower porosity or strengthen the material's structural integrity can be evaluated.

Table 4: Porosity size improvement (Pre-Optimization)

Pre-Optimization No of Porosity in 56 mm 9	Size in mm
1	2.1
2	2.3
3	2.5
4	2.4
5	2.8
6	2.9
7	3.1
8	3.2
9	3.3

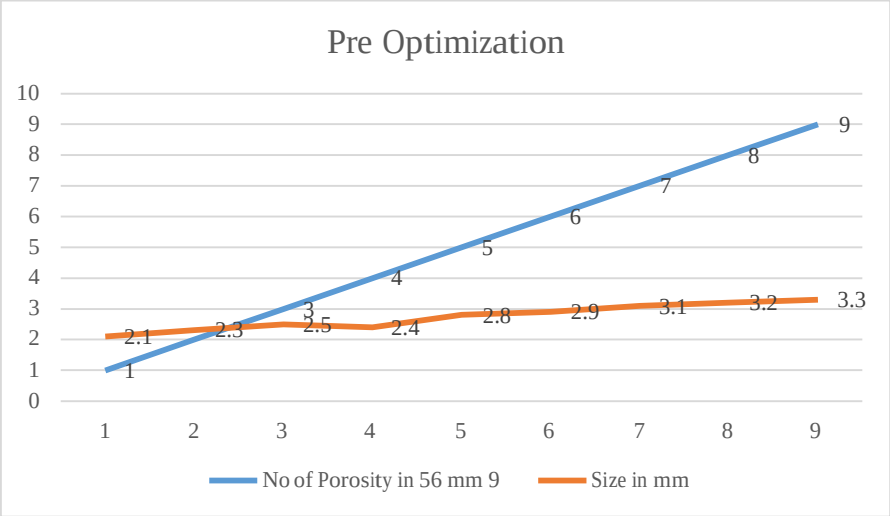

Figure 8: Pre optimization in porosity

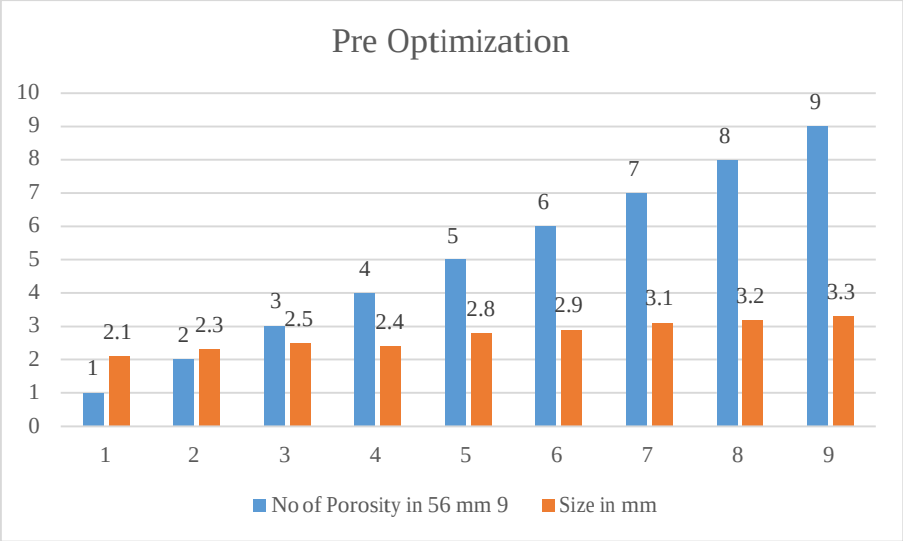

Figure 9: Graphical representation of Pre optimization in porosity

Post-optimization statistics on the porosity properties of a 56 mm-diameter material are shown in Table 5 and figure 10 and figure 11. Nine distinct porosity sizes, expressed in millimeters, are included in the table. The sizes of the pores vary from 0.5 mm to 1.5 mm. Nine different porosities have been found in the substance, according to the data. The porosity sizes range from 0.5 mm to 1.5 mm, with the smallest size being stated first and the largest size being listed last. These dimensions are, in exact order, as follows: 0.5 mm, 0.6 mm, 0.7 mm, 0.8 mm, 0.9 mm, 1.2 mm, 1.3 mm, 1.4 mm, and 1.5 mm. This data points to the need for a thorough examination of the porosity distribution of the material, which can be essential to comprehending both its structural characteristics and its uses.

Table 5: Porosity size improvement (Post-Optimization)

Post-Optimization No of Porosity in 56 mm 9	Size in mm
1	0.5

2	0.6
3	0.7
4	0.8
5	0.9
6	1.2
7	1.3
8	1.4
9	1.5

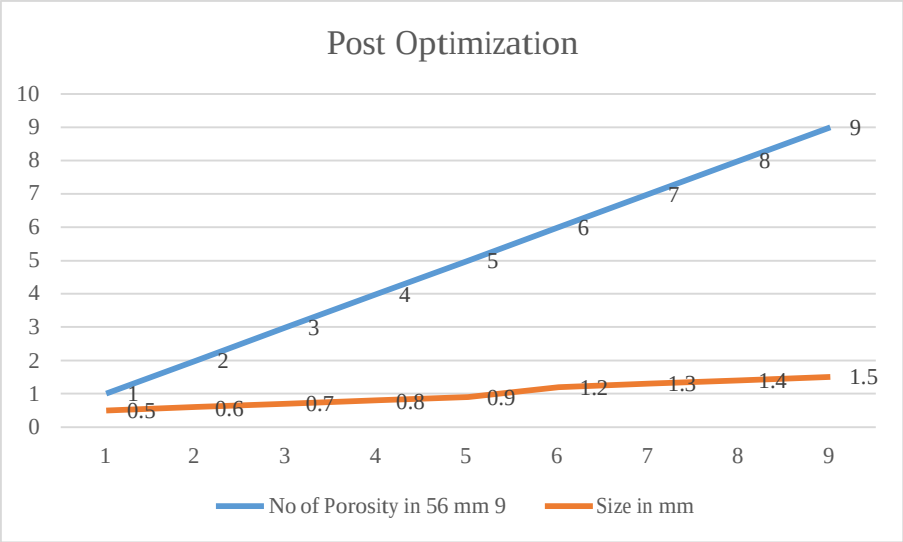

Figure 10: Post optimization in porosity

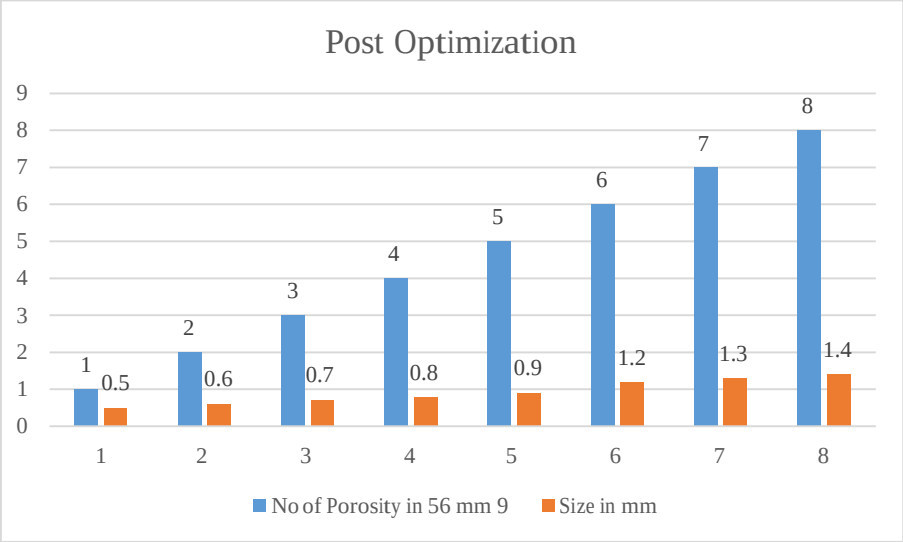

Figure 11: Graphical representation of Post optimization in porosity

4.1 Optimization Findings

A comparison of different process parameters before and after optimization is shown in Table 6. Specific units of measurement are used to categorize and measure the parameters (UOM). The holding furnace temperature for Category A was raised from 640 degrees Celsius (°C) prior to optimization to 700 degrees Celsius (°C) following optimization. The die temperature in Category B increased from 185°C to 195°C, which is also expressed in degrees Celsius (°C). Category C deals with the first stage projectile velocity, which is expressed in meters per second (m/s). After the optimization procedure, this velocity rose to 0.23 m/s from 0.12 m/s. In the second stage, the plunger velocity increased significantly from 0.32 m/s to 2.5 m/s, comparable to Category D. This increase was also measured in meters per second (m/s). Finally, Category E delineates the amplified pressure in bars during the third stage. The optimal pressure was increased from 130 bars to 285 bars. These modifications demonstrate substantial improvements in the process parameters, which have the potential to enhance the system's overall performance and efficacy.

Table 6: Process parameter pre and post optimizations

Category	PP	UOM	Pre optimization	Post optimization
A	Holding furnace temperature	C˚	640	700
B	Die temperature	C˚	185	195
C	Plunger velocity 1st stage	m/s	0.12	0.23
D	Plunger velocity 2nd stage	m/s	0.32	2.5
E	Multiplied pressure 3rd stage	Bar	130	285

The highest force and related elongation at break for a series of tests on materials carried out before the application of any optimization processes are shown in table 7, "Pre-Optimization Break Load". The two primary columns in the table are "F max Kn" and "E Break mm."The maximum force applied in kilonewtons (Kn) that each material sample could withstand before breaking is shown in the "F max Kn" column. Following testing, the maximum forces of four samples were noted as follows: 10.70 kg, 10.90 kg, 12.90 kg, and 7.90 kg. The elongation at break in millimeters (mm), or the amount that each material sample extended before failing, is displayed in the "E Break mm" column. The four samples had recorded elongation values of 0.68 mm, 0.5 mm, 0.91 mm, and 0.69 mm, in that order. These findings give an overview of the material's mechanical characteristics prior to optimization, emphasizing the range in the forces they can sustain as well as their breaking point elongation capacities. This

information is necessary to comprehend the materials' baseline performance, which is important for comparison once optimization attempts are made.

Figure 12: Porosity Level 3 Break load 10.90 KN

They examined four different parts, with Level 3 porosity and Level 4 porosity observed. The corresponding break load tests were 12, 7, 9, 10, 70, and 10. 90 KN, as shown in figure 12. Electrical fuses are used to guard against overcurrent damage to electrical circuits. Within them is a metal strip that, in the event of an excessive current flow, melts, breaking the circuit and safeguarding the other components. The cartridge fuse is connected to the circuit through the holes in it. "L3-Break load 10.90," which appears on the fuse, most likely relates to the kind and rating of the fuse. "L3" may refer to a specific circuit, and "Break load 10.90" may denote the highest current that the fuse can manage prior to the circuit breaking.

Table 7: Pre optimization break load

S.No.	F max Kn	E Break mm
1.	12.00	0.68
2.	7.90	0.5
3.	10.70	0.91
4.	10.90	0.69

Table 8: Post optimization break load

S.No.	F max Kn	E Break mm
1.	21.22	0.99
2.	28.00	0.95
3.	22.23	0.96
4.	24.79	1.23

The post-optimization break load data for several samples are shown in Table 8. The first sample had an extension at break of 0.99 mm and a maximum force of 21.22 kN. In contrast to the first sample, the second sample exhibited a slightly lower extension at break of 0.95 mm but a greater maximum force of 28.00 kN, suggesting that it could withstand more force before breaking. With a little greater force and a significantly lower extension, the third sample showed similar characteristics to the first sample. Its maximum force was 22.23 kN, and its extension at break was 0.96 mm. The fourth sample demonstrated a moderate force resistance with the highest extension among the four samples, with a maximum force of 24.79 kN and an extension at break of 1.23 mm. Overall, the evidence points to variations in the samples post-optimization break load performance, which are reflected in variations in their maximum force and extension at break.

Table 9: Breakfast load improvement (Pre-Optimization)

Pre-Optimization Load in kN	Elongation mm
12	0.68

7.9	0.5
10.7	0.91
10.9	0.69

Data from a pre-optimization stage of a structural or material testing procedure are shown in Table 9 and figure 13. For four separate cases, it provides the applied load in kilonewtons (kN) and the corresponding elongation in millimeters (mm). In particular, the material elongates by 0.68 mm at a force of 12 kN. In a similar vein, the elongation is 0.5 mm with a force of 7.9 kN. The elongation is measured at 0.91 mm when the load reaches 10.7 kN and 0.69 mm when the load reaches 10.9 kN. This information is essential for comprehending how the material behaves under various loads, which can help with decision-making regarding the optimization and enhancement of the material's structural integrity and performance.

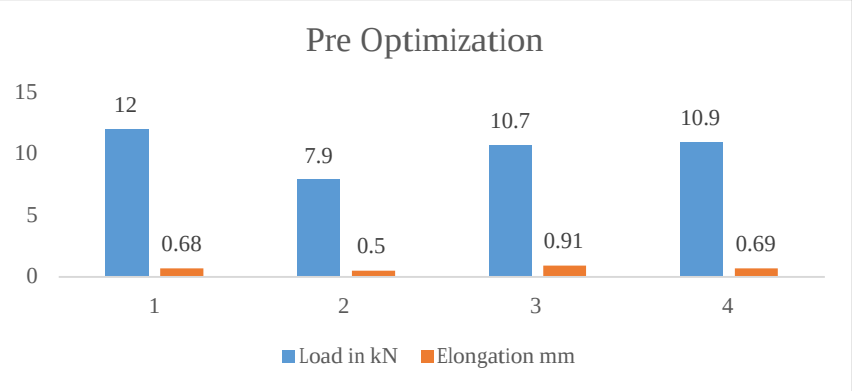

Figure 13: Graphical representation of Breakfast load improvement (Pre-Optimization)

Table 10: Breakfast load improvement (Post-Optimization)

Post-Optimization Load in kN	Elongation mm
21.22	0.99
28	0.95
22.23	0.96
24.79	1.23

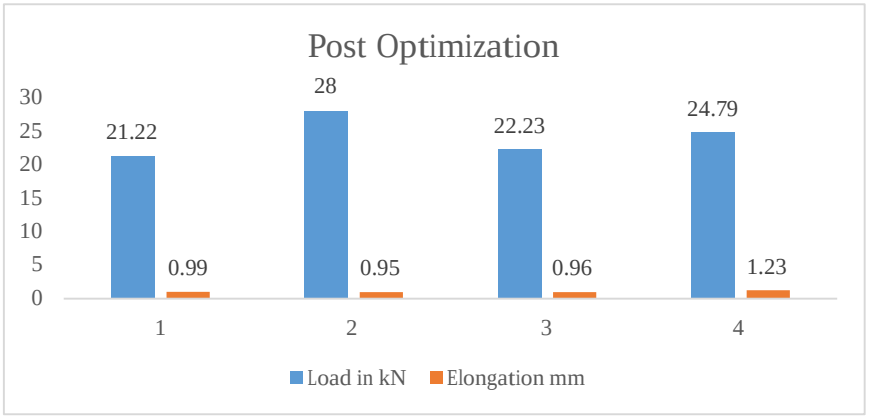

Figure 14: Graphical representation of Breakfast load improvement (post-optimization)

Data on the post-optimization load and related elongation measurements are shown in Table 10 and figure 14. Following an optimization procedure, the load values, expressed in kilonewtons (kN), and the elongation, expressed in millimeters (mm), show how a material or structure behaves under various loading circumstances. In particular, the first row shows that an elongation of 0.99 mm is produced by a force of 21.22 kN. The second row exhibits a significantly smaller elongation of 0.95 mm due to a higher load of 28 kN. Like the previous load but with a somewhat smaller elongation, a load of 22.23 kN in the third-row results in an elongation of 0.96 mm. The last row shows that a load of 24.79 kN results in a 1.23 mm elongation, which is noticeably bigger. This change in elongation in response to varying loads emphasizes the mechanical qualities of the material or structure's flexibility as well as the impact of the optimization process.

CONCLUSION

The optimized parameters resulted in improved tensile strength, reduced porosity, and enhanced overall structural integrity of the castings. The study demonstrates that DOE is an effective approach for optimizing HPDC processes, leading to consistent production of high-quality $AlSi_9$ Cu_3 alloy components. The findings underscore the importance of precise control over casting parameters and provide a robust framework for further improvements and applications in the die casting industry. This study investigated the impact of die casting process parameters on the formation of porosity in rectangular die castings of the aluminum alloy $AlSi_9Cu_3$ in a real industrial setting by employing precise and high-performance equipment. The primary goal of this investigation was to establish guidelines for the application of the Genetic Algorithm technique in the die casting process. Consequently, die casting specialists will find it simpler to learn and implement, as the method's complexity has been intentionally minimized. The primary determinants of the casting porosity of $AlSi_9Cu_3$ aluminum alloy castings in the first, second, and third stages died temperature, multiplication pressure, projectile velocity, and holding furnace temperature. They demonstrate that genetic algorithms are capable of accurately predicting the intricate relationship between the parameters of the die casting process and the formation of porosity in castings composed of $AlSi_9Cu_3$ aluminum alloy. This offers an enhanced model for the pressure die casting procedure that yields outstanding results. The experimental data robustly validates both the minimal porosity estimate by GA and the expected process parameter values. Furthermore, the suggested modeling and optimization approaches hold significant promise for challenging industrial applications such as pressure die casting.

Author contribution

Vinod Kumar Verma conducted the research as a Research Scholar under the guidance of Professor Sanjeev Sharma (corresponding author). Sandeep Phogat provided additional expertise as an Assistant Professor. Professor Ajay Kumar Mishra offered insights from the Academy of Nanotechnology, while PB Sharma, the Vice Chancellor, lent their overall support to the research project.

Acknowledgements

The authors would like to express their sincere gratitude to the Department of Mechanical Engineering at Amity University Gurugram for providing the necessary resources and facilities to conduct this research. Special thanks to Prof. Sanjeev Sharma for his invaluable guidance and support throughout the study. We also appreciate the contributions of Dr. Sandeep Phogat and Prof. Ajay Kumar Mishra for their assistance with data analysis and methodological insights. We are grateful to Vice Chancellor PB Sharma for his encouragement and support. Finally, we acknowledge the critical feedback provided by the anonymous reviewers, which greatly enhanced the quality of this work.

Competing interest

The author declares that there is no competing interest.

Funding

There is no funding statement.

Conflict of interest

There is no conflict of interest.

REFERENCES

1. Verran GO, Mendes RPK, Dalla Valentina LV. (2008). DOE applied to optimization of aluminum alloy die castings. Journal of materials processing technology, 200(1-3), 120-125.
2. Adamane AR, Arnberg L, Fiorese E, Timelli G, Bonollo F. (2015). Influence of injection parameters on the porosity and tensile properties of high-pressure die cast Al-Si alloys: A review. International journal of metalcasting, 9, 43-53.
3. Adke MN, Karanjkar SV. (2015). Optimization of die-casting process parameters using DOE. Int. J. Eng. Res. Gen. Sci, 3(2), 1314-25.
4. Do TA, Tran VT. (2018). Optimization of Precision Die Design on High-Pressure Die Casting of AlSi 9 Cu 3. In Proceedings of the Computational Mechanics 2017: ACOME 2017, 2 to 4 August 2017, Phu Quoc Island, Vietnam (pp. 759-771). Springer Singapore.
5. Hsu QC, Do AT. (2013). Minimum porosity formation in pressure die casting by Taguchi method. Mathematical Problems in Engineering, 2013(1), 920865.
6. Apparao KC, Birru AK. (2017). Optimization of Die casting process based on Taguchi approach. Materials Today: Proceedings, 4(2), 1852-1859.
7. Patel GM, Krishna P, Parappagoudar MB. (2014). Optimization of squeeze cast process parameters using Taguchi and grey relational analysis. Procedia Technology, 14, 157-164.
8. Apparao, K.C. and Birru, A.K., 2017. Optimization of Die casting process based on Taguchi approach. Materials Today: Proceedings, 4(2), pp.1852-1859.
9. Santhosh AJ, Lakshmanan AR. (2016). Investigation of ductile iron casting process parameters using Taguchi approach and response surface methodology. China Foundry, 13, 352-360.
10. Ubani NO, Nwobi-Okoye CC, Dara JE, Eni-Ikeh SN, Okoro C. (2023). Optimization approach for evaluation of mechanical properties of high pressure die cast aluminum alloyed product. Umudike Journal of Engineering and Technology, 9(1), 46-54.
11. Rosnitschek T, Erber M, Hartmann C, Volk W, Rieg F, Tremmel S. (2021). Combining Structural Optimization and Process Assurance in Implicit Modelling for Casting Parts. Materials 2021, 14, 3715.
12. Anilchandra AR, Arnberg L, Bonollo F, Fiorese E, Timelli G. (2017). Evaluating the tensile properties of aluminum foundry alloys through reference castings—a review. Materials, 10(9), 1011.
13. Chavan CV, Pawar PJ. (2013). Parametric Optimization of Die Casting Process using Cuckoo Search Algorithm. Dr. R. Venkata Rao, 51.
14. Outmani I, Fouilland-Paille L, Isselin J, El Mansori M. (2017). Effect of Si, Cu and processing parameters on Al-Si-Cu HPDC castings. Journal of Materials Processing Technology, 249, 559-569.
15. Shahria S, Tariquzzaman M, Rahman MH, Al Amin M, Rahman MA. (2017). Optimization of molding sand composition for casting Al alloy. International Journal of Mechanical Engineering and Applications, 5(3), 155-161.
16. Rathinam N, Dhinakaran R, Sharath E. (2021). Optimizing process parameters to reduce blowholes in high pressure die casting using Taguchi methodology. Materials Today: Proceedings, 38, 2871-2877.

17. Chandrasekaran R, Campilho RDSG, Silva FJG. (2019). Reduction of scrap percentage of cast parts by optimizing the process parameters. Procedia Manufacturing, 38, 1050-1057.
18. Balikai VG, Siddlingeshwar IG, Gorwar M. (2018). Optimization of process parameters of High Pressure Die Casting process for ADC12 Aluminium alloy using Taguchi method. Int. J. Pure Appl. Math, 120(6), 959-969.
19. Cica D, Kramar D. (2018). Intelligent process modeling and optimization of porosity formation in high-pressure die casting. International Journal of Metalcasting, 12, 814-824.
20. Rao RV, Rai DP. (2017). Optimization of selected casting processes using Jaya algorithm. Materials Today: Proceedings, 4(10), 11056-11067.
21. Vicario I, Anza I, Tejada F, Alonso J, Galarraga H, Merchan M. (2014, May). Development of new Al-Si9Cu3 alloys for HPDC components with tailored properties. In Proceedings of the 71st World Foundry Congress: Advanced Sustainable Foundry, Bilbao, Spain (pp. 19-21).
22. Wang L, Turnley P, Savage G. (2011). Gas content in high pressure die castings. Journal of Materials Processing Technology, 211(9), 1510-1515.